STM JOURNALS

Journal of
Polymer & Composites

ISSN: 2321-2810 (Online)
ISSN: 2321-8525 (Print)
Volume 13, Issue 6, 2025
DOI (Journal): 10.37591/JoPC

https://journals.stmjournals.com/jopc/

Research JoPC

Aluminium-Doped Zinc Ferrite Nanoparticles Synthesized by Combustion Method for Polymer Composite Applications

A. Roniboss[1,*], P. Vani[2], S. Sumathi[3], K. Umavathy[4], Partha Sarathi Subudhi[5], R. Revathi[6], M. Sundararajan[7], Chandra Sekhar Dash[8], S. Yuvaraj[9], G. Suresh[10]

Abstract

$ZnFe_{2-x}Al_xO_4$ ($x = 0$ and 0.5) nanoparticles were synthesized via a combustion method owing to its simplicity, cost efficiency, and ability to produce highly crystalline nanomaterials. Powder X-ray diffraction (XRD) analysis confirmed the formation of a single-phase cubic spinel structure without detectable secondary phases, indicating high phase purity. The average crystallite size was estimated to be in the range of 14–20 nm, confirming the nanocrystalline nature of the samples. Field-emission scanning electron microscopy (FE-SEM) revealed nearly spherical and uniformly distributed particles, while energy-dispersive X-ray spectroscopy (EDX) confirmed the elemental composition and successful incorporation of Al^{3+} ions into the $ZnFe_2O_4$ lattice. Fourier transform infrared (FTIR) spectra exhibited characteristic metal–oxygen stretching vibrations associated with tetrahedral and octahedral sites, further validating the formation of spinel ferrite structures.

Optical absorption studies demonstrated a slight reduction in the optical band gap from 1.81 eV to 1.75 eV with Al substitution, which can be attributed to modified electronic transitions within the lattice. Furthermore, a systematic annealing study was conducted on co-precipitated Al-doped zinc ferrite nanoparticles to examine the influence of thermal treatment on structural stability and functional properties. Magnetic measurements performed using vibrating sample magnetometry (VSM) indicated soft ferromagnetic behavior with low coercivity, highlighting their suitability for low-power magnetic applications. The coexistence of semiconducting optical characteristics and soft ferromagnetism underscores the multifunctional nature of the $ZnFe_{2-x}Al_xO_4$ nanoparticles. These results demonstrate their potential application as effective nanofillers in polymer-based multifunctional composites for magnetic storage, optoelectronic, and spintronic devices.

***Author for Correspondence**
A. Roniboss
E-mail: roniboss8@gmail.com

[1]Assistant Professor, Department of Chemistry, Vel Tech Rangarajan Dr. Sagunthala R&D Institute of Science and Technology, Vel Nagar, Avadi, Chennai, Tamil Nadu, India.
[2]Assistant Professor, Department of Physics, Vel Tech Rangarajan Dr. Sagunthala R&D Institute of Science and Technology, Vel Nagar, Avadi, Chennai, Tamil Nadu, India.
[3]Associate Professor, Department of Chemistry, Sri Sairam Engineering College, Chennai, Tamil Nadu, India.
[4]Assistant Professor, Department of Chemistry, Immaculate College for Women, Cuddalore, Tamil Nadu, India.
[5]Assistant Professor, Department of Electrical Engineering, Bajaj Institute of Technology, Wardha, Maharashtra, India
[6]Assistant Professor, Department of Biotechnology, Periyar University Centre for Postgraduate and Research Studies, Dharmapuri, Tamil Nadu, India.
[7]Assistant Professor, PG & Research Department of Physics, Paavendhar College of Arts & Science, M.V. South, Thalaivasal, Salem, Tamil Nadu, India
[8]Associate Professor, Department of Electronics and Communication Engineering, Centurion University of Technology and Management, Bhubaneswar, Odisha, India.
[9]Associate Professor, Department of Physics, Vel Tech Rangarajan Dr. Sagunthala R&D Institute of Science and Technology, Vel Nagar, Avadi, Chennai, Tamil Nadu, India.
[10]Professor, Department of Mathematics, Vel Tech High Tech Dr.Rangarajan Dr.Sakunthala Engineering College, Chennai, Tamil Nadu, India

Received Date: August 20, 2025
Accepted Date: November 12, 2025
Published Date: December 23, 2025

Citation: A. Roniboss, P. Vani, S. Sumathi, K. Umavathy, Partha Sarathi Subudhi, R. Revathi, M. Sundararajan, Chandra Sekhar Dash, S. Yuvaraj, G. Suresh. Aluminium-Doped Zinc Ferrite Nanoparticles Synthesized by Combustion Method for Polymer Composite Applications. Journal of Polymer & Composites. 2025; 13(6): 272–282p.

Keywords: $ZnFe_2O_4$ nanoparticles; Trivalent dopant; Combustion synthesis; Optical Band gap; polymer composites;

INTRODUCTION

Magnetic nanomaterials, particularly spinel ferrites, have garnered considerable attention due to their unique nanoscale behavior and wide-ranging applications. The nanoscale reduction in particle size leads to phenomena such as single-domain magnetism, quantum size effects, and an enhanced surface-to-volume ratio attributes that significantly boost their magnetic performance compared to bulk counterparts [1–3]. Among these, spinel ferrites with the general formula MFe_2O_4 are soft magnetic materials known for their tunable physical properties, making them attractive for integration into polymer composite systems for use in sensors, electromagnetic shielding, and energy applications [4-7].

Zinc ferrite ($ZnFe_2O_4$) is a particularly important member of this family, exhibiting room-temperature magnetic behavior and a normal spinel structure, with Zn^{2+} ions occupying tetrahedral (A) sites and Fe^{3+} ions occupying octahedral (B) sites [8]. Although $ZnFe_2O_4$ typically shows antiferromagnetic characteristics, its properties can be engineered through ionic substitution. Recent efforts have focused on doping $ZnFe_2O_4$ with various divalent and trivalent cations (e.g., Mg^{2+}, Ca^{2+}, Dy^{3+}, Mn^{2+}, Cu^{2+}) to enhance photocatalytic efficiency, magnetic responsiveness, and electrical behavior—making these nanoparticles viable candidates for inclusion in polymer matrices for advanced composite materials [9].

For example, Rayees Ahamed et al. reported that Mg doping induces weak ferromagnetism in $ZnFe_2O_4$ nanoparticles, making them suitable for magnetic sensors, nanomedicine, and optoelectronic applications [10]. Yaseen Ahamed et al. demonstrated that Ca and Dy co-doping increased the optical band gap and magnetic softness, while decreasing crystallite size features that can improve dispersion and functionality in polymer nanocomposites [11]. Aamir Mahmood et al. showed that Mn substitution leads to large polaron tunneling conduction behavior, supporting their use in electronic and dielectric polymer composites [12]. Their studies also demonstrated improved microwave absorption properties in Mn and Cu-doped $ZnFe_2O_4$, suggesting relevance for electromagnetic interference shielding in polymer-based devices [13].

Notably, aluminum doping (Al^{3+}) has shown significant promise for enhancing the physical characteristics of spinel ferrites. It improves charge mobility, crystallinity, and resistivity, while also lowering dielectric losses—making Al-doped $ZnFe_2O_4$ suitable as multifunctional fillers in polymer matrices for use in magnetic, dielectric, and photocatalytic applications [14]. The introduction of trivalent Al^{3+} ions can also influence the biological compatibility of ferrite materials, extending their relevance to biomedical polymer composites.

Zinc ferrite ($ZnFe_2O_4$) was chosen as the base material because of its multifunctional physical properties and excellent compatibility with polymers. It is a soft magnetic spinel oxide with adjustable magnetic characteristics, which are beneficial in electromagnetic shielding, microwave absorption, and sensing applications. In addition, $ZnFe_2O_4$ exhibits good chemical stability, environmental safety, and moderate electrical resistivity, making it an effective candidate for polymer reinforcement. Its nanoparticle form provides high surface activity, improving interfacial interaction with polymers and enabling diverse applications in electronic and photonic devices [15]. This study presents a systematic investigation of the structural modifications induced by annealing in Al-doped $ZnFe_2O_4$ nanoparticles synthesized via co-precipitation. Emphasis is placed on understanding how thermal treatment affects crystallinity, particle morphology, and magnetic behavior key parameters for the performance of polymer nanocomposites. By correlating microstructural evolution with functional enhancements, this research aims to guide the development of optimized Al-doped zinc ferrite nanofillers for next-generation polymer-based composite applications in magnetic, optoelectronic, and biomedical fields.

MATERIAL SYNTHESIS AND METHODOLOGY

Materials and Reagents

All the chemicals used for this study, including aluminium nitrate, L-alanine, iron(III) nitrate, and zinc(II) nitrate, were of scientific grade (≥99%) and purchased from Merck, (India). No additional purification steps were performed. Deionized water was utilized for all sample preparations.

Experimental Approach

The synthesis of $ZnFe_2O$ -xAl_xO_4 (x = 0 & 0.5) nanoparticles involved dissolving stoichiometric amounts of zinc nitrate, aluminum nitrate, iron nitrate, and L-alanine in deionized water, followed by stirring for an hour at ambient temperature. The homogeneous solution was heated at 100 degrees centigrade for 10 minutes in a hot air oven, utilizing nitrates as oxidizers, which facilitate combustion or burning reactions and L-alanine as combustion fuel with a fuel-to-oxidizer ratio of one. This combustion process involved sequential boiling, dehydration, decomposition, gas evolution, and spontaneous ignition, ultimately producing solid, fluffy $ZnFe_2$-xAl_xO_4 nanoparticles. The as-obtained samples were thermally treated at 570 degrees centigrade for 90 min with a temperature ramp of 5°C/min. The resulting samples were labelled as follows: $ZnFe_2O_4$ (x = 0) as Sample (a) and $Al_{0.5}ZnFe_{1.5}O_4$ (x = 0.5) as Sample (b).

Characterization techniques

The structural, morphological, and magnetic properties of $ZnFe_2O_{-x}Al_xO_4$ (x = 0, 0.5) nanoparticles were characterized using various techniques. The structural properties of the samples were analyzed using X-ray diffraction (XRD) on a Rigaku Ultima IV diffractometer. Morphological analysis was performed using field emission scanning electron microscopy (FE-SEM) and energy dispersive X-ray (EDX) spectroscopy on a Joel JSM 6360 instrument. Optical properties were investigated using Thermo Scientific Evolution 300 UV-Vis and Nicolet iS 10 FT-IR spectrophotometers. Magnetic properties were measured at room temperature (300 K) using a Lakeshore VSM 7410 vibrational sample magnetometer equipped with 3 Tesla magnets.

RESULT AND DISCUSSION

Powder X-Ray Diffraction Analysis (XRD)

Figure 1 presents the X-ray diffraction (XRD) patterns of $ZnFe_2O_{-x}Al_xO_4$ (x = 0, 0.5) spinel nanoparticles, confirming their crystalline nature. The diffractogram exhibit peaks at 2θ values of 30.10˚, 35.69˚, 43.19˚, 54.02˚, 57.40˚, and 62.61˚. These peak position correspond to (220), (311), (400), (422), (511), and (440) hkl values respectively, which are characteristic of zinc ferrite (JCPDS card no. 89-4926). These reflections indicate a cubic structure of spinel ferrites with Fd-3m space group [16-17] which is critical for maintaining magnetic and dielectric consistency when these nanoparticles are embedded in polymer matrices. The average crystallite size (L) was calculated using the Debye-Scherrer equation (Eq. 3.1) based on the (311) reflection peak.

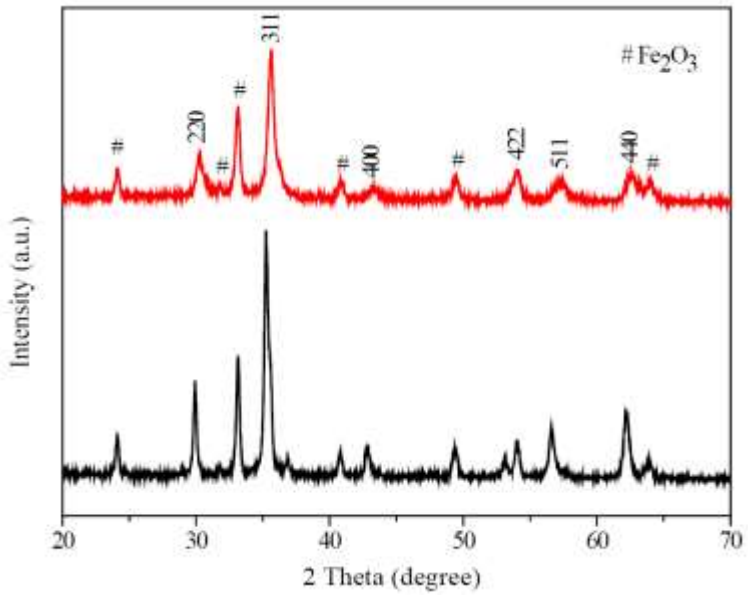

Figure 1. XRD patterns of $ZnFe_{2-x}Al_xO_4$ (x = 0 and 0.5) nanoparticles.

Table 1. Sample name, sample code, crystallite size, lattice parameter and band gap values of $ZnFe_{2-x}Al_xO_4$ (x = 0.0 and 0.5) samples.

Sample name	Sample code	Crystallite Size, L (nm)	Lattice Parameter, a=b=c (Å)	Energy gap (eV)
$ZnFe_2O_4$	a	14	8.387	1.81
$ZnFe_{1.5}Al_{0.5}$ Fe_2O_4	b	20	8.395	1.75

$$L = \frac{0.89\lambda}{\beta \cos\theta} \tag{3.1}$$

which relates L to the X-ray wavelength (λ = 0.15406 nm), the full width at half maximum (FWHM) of the diffraction peak (β), and the diffraction angle (θ). The calculated average crystallite sizes of $ZnFe_2O$-xAl_xO_4 nanoparticles, based on the (311) diffraction peak, revealed values of approximately 14 nm for x = 0 and 20 nm for x = 0.5.

From, Eq. 3.2, the lattice parameter (*a*) of the $ZnFe_2O_{-x}Al_xO_4$ (*x* = 0 and 0.5) nanoparticle is calculated

$$a = d_{hkl}\sqrt{(h^2 + k^2 + l^2)} \tag{3.2}$$

where, d_{hkl}, the inter-atomic spacing with respect to the h, k, and l miller indices of the crystal planes. Table 1 confirms the cubic spinel structure of the synthesized pure and aluminium-doped $ZnFe_2O_4$ nanoparticles through their lattice parameter values, which are 8.387 Å for $ZnFe_2O_4$ and 8.395 Å for $ZnFe_{1.5}Al_{0.5}O_4$, respectively.

Field Emission Scanning Electron Microscopy Analysis (FESEM)

The morphological characteristics of $ZnFe_{2-x}Al_xO_4$ (x = 0 and 0.5) nanoparticles were thoroughly examined using field emission scanning electron microscopy (FE-SEM) to evaluate their suitability for composite integration. As shown in Figure 2, both undoped and Al-doped $ZnFe_2O_4$ nanoparticles exhibit a predominantly spherical morphology with relatively uniform particle sizes. Numerous fine, spherical structures were observed, and these nanoparticles tend to form loosely bound aggregates, indicating strong interparticle interactions. Such aggregation behavior can play a critical role in determining the dispersion quality and interfacial bonding of the nanoparticles within polymer matrices. The observed surface topography and morphology suggest good potential for these nanoparticles to serve as functional fillers in polymer composite systems, where controlled morphology can significantly influence mechanical strength, magnetic responsiveness, and dielectric behavior. The FE-SEM analysis thus offers valuable insights into the structural features that govern their performance in composite material applications.

Energy Dispersive X-Ray Spectroscopy Analysis (EDAX)

The elemental constituents of the prepared $ZnFe_2O$-xAl_xO_4 (x = 0 and 0.5) nanoparticles was profiled using EDX. Figure 3 spectra provides both qualitative and quantitative information about the elements present in the nanoparticles. The EDX histogram (Figure 3) displays the elemental profile of the synthesized nanoparticles, revealing the presence of zinc (Zn), aluminium (Al), iron (Fe), and oxygen (O) as the primary constituents. Further analysis of the EDX spectra confirms that these elements are integral components of the $ZnFe_2$-xAl_xO_4 nanoparticles Figure 4(a)–(d) and 5(a)–(e) display the elemental mapping images of $ZnFe_2O_4$ and $ZnAl_{0.5}Fe_{1.5}O_4$ spinel nanoparticles, respectively. The elemental maps in Figure 4(a)–(d) reveal the distribution of zinc (Zn), iron (Fe), and oxygen (O) atoms within the $ZnFe_2O_4$ nanoparticles. Similarly, the elemental maps in Figure 5 (a)–(e) confirm the presence and distribution of zinc (Zn), aluminum (Al), iron (Fe), and oxygen (O) atoms in the $ZnAl_{0.5}Fe_{1.5}O_4$ nanoparticles.

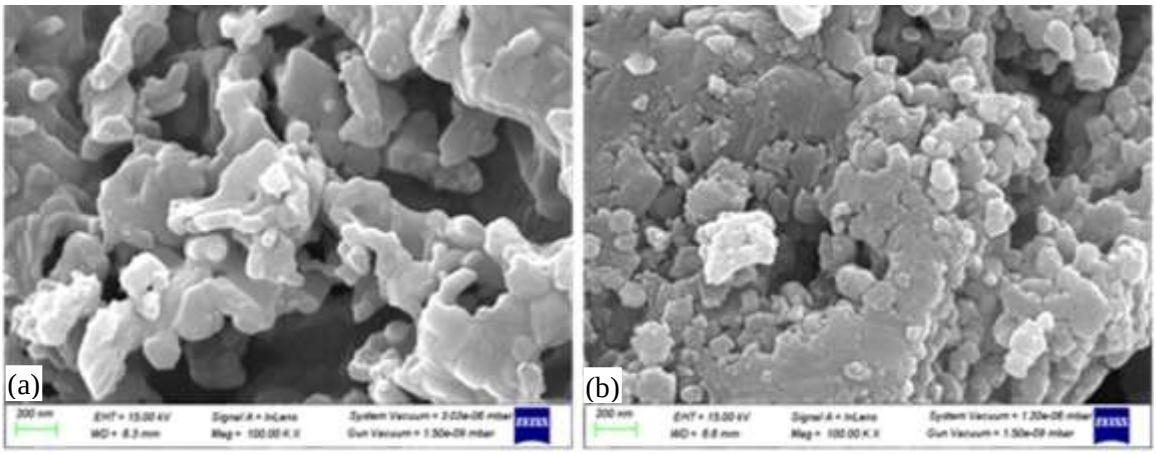

Figure 2. FE-SEM image of $ZnFe_{2-x}Al_xO_4$ (x = 0 and 0.5) nanoparticles.

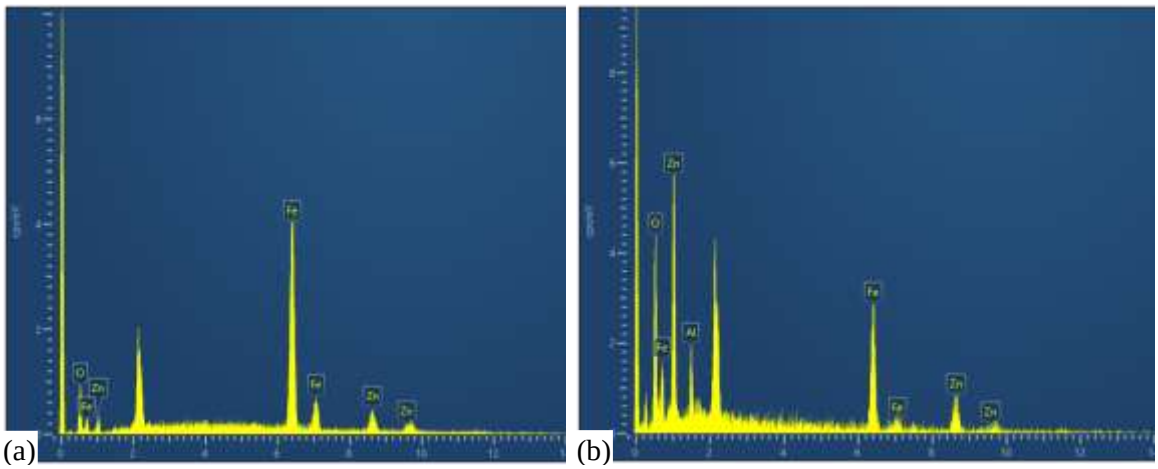

Figure 3. EDX spectra of $ZnFe_{2-x}Al_xO_4$ (x = 0 and 0.5) nanoparticles.

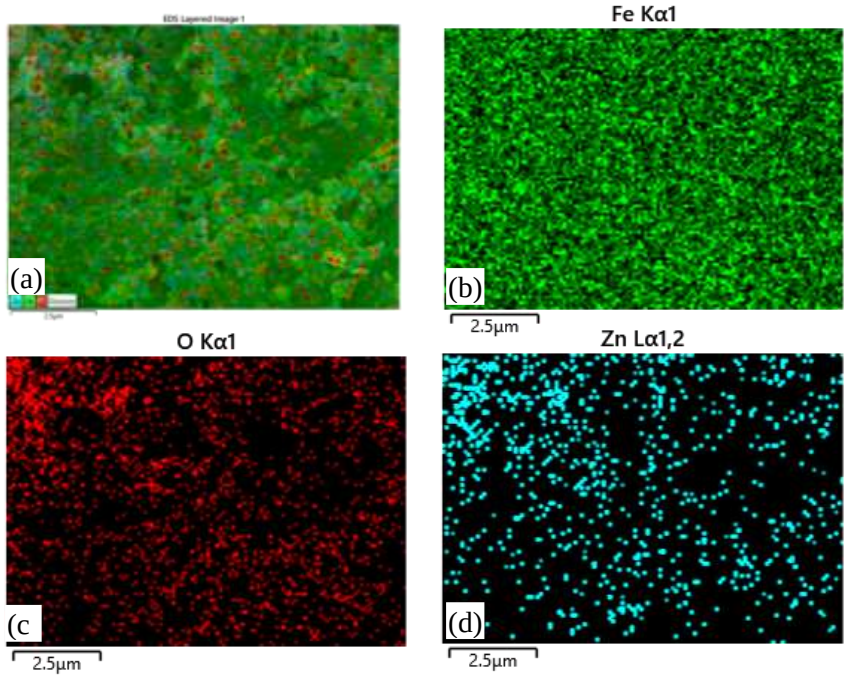

Figure 4. (a)–(d) Mapping spectra of $ZnFe_{2-x}Al_xO_4$ (x = 0) nanoparticles.

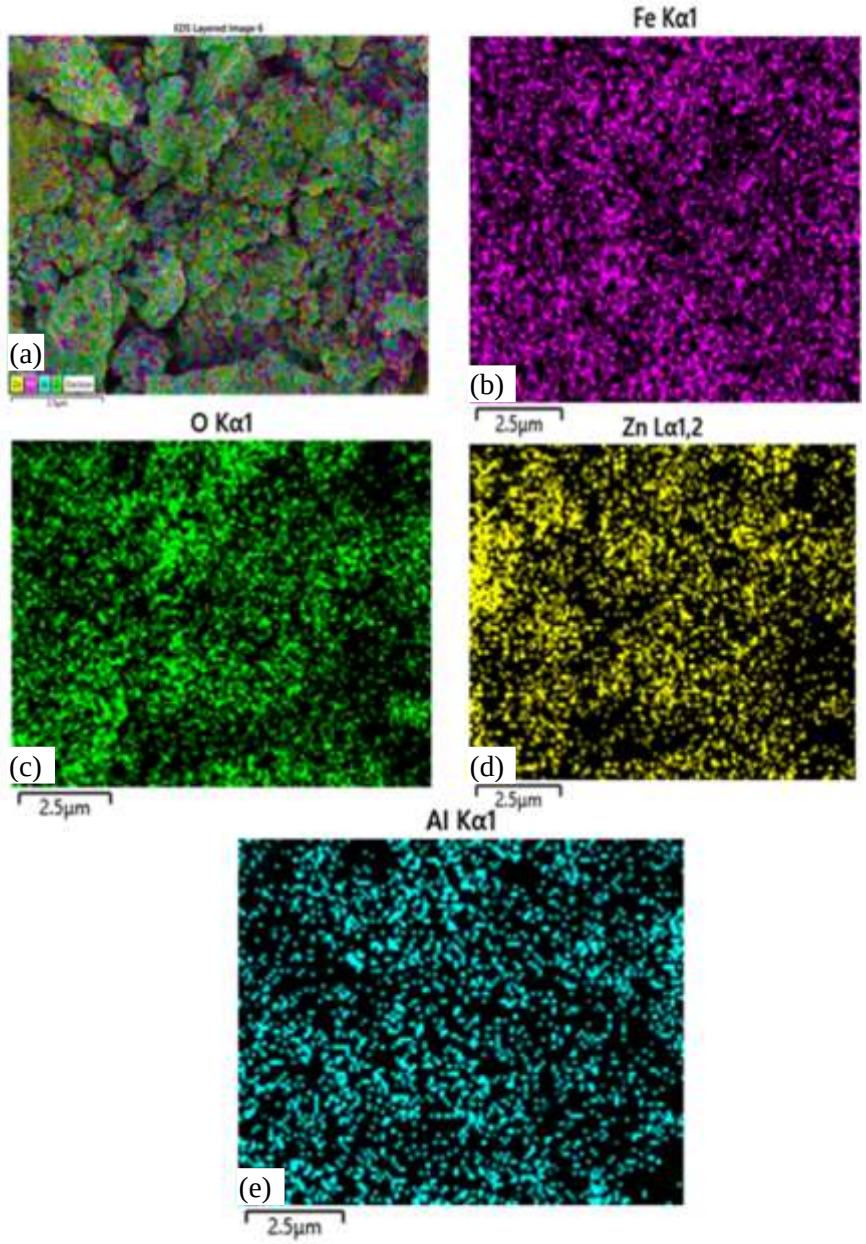

Figure 5. (a)–(e) Mapping spectra of $ZnFe_{2-x}Al_xO_4$ (x = 0.5) nanoparticles.

UV-Visible Absorption Study Analysis

The optical band gap of $ZnFe_{2-x}Al_xO_4$ (x = 0 and 0.5) nanoparticles was determined using the Tauc relation, where the Kubelka-Munk function converted reflectance data to absorption coefficients, as described by equation (3.3).

$$\propto = F(R) = \frac{(1-R)^2}{2R} \tag{3.3}$$

The Kubelka-Munk function, F(R), is related to the absorption coefficient (α) and reflectance (R). The Tauc relation, expressed in equation (3.4), is used to determine the optical bandgap energy.

$$F(R)hv = A(hv - E_g)^n \tag{3.4}$$

The values of n, specifically 1/2 and 2, represent allowed direct and indirect electronic transitions, providing a way to determine the distinct bandgap values.

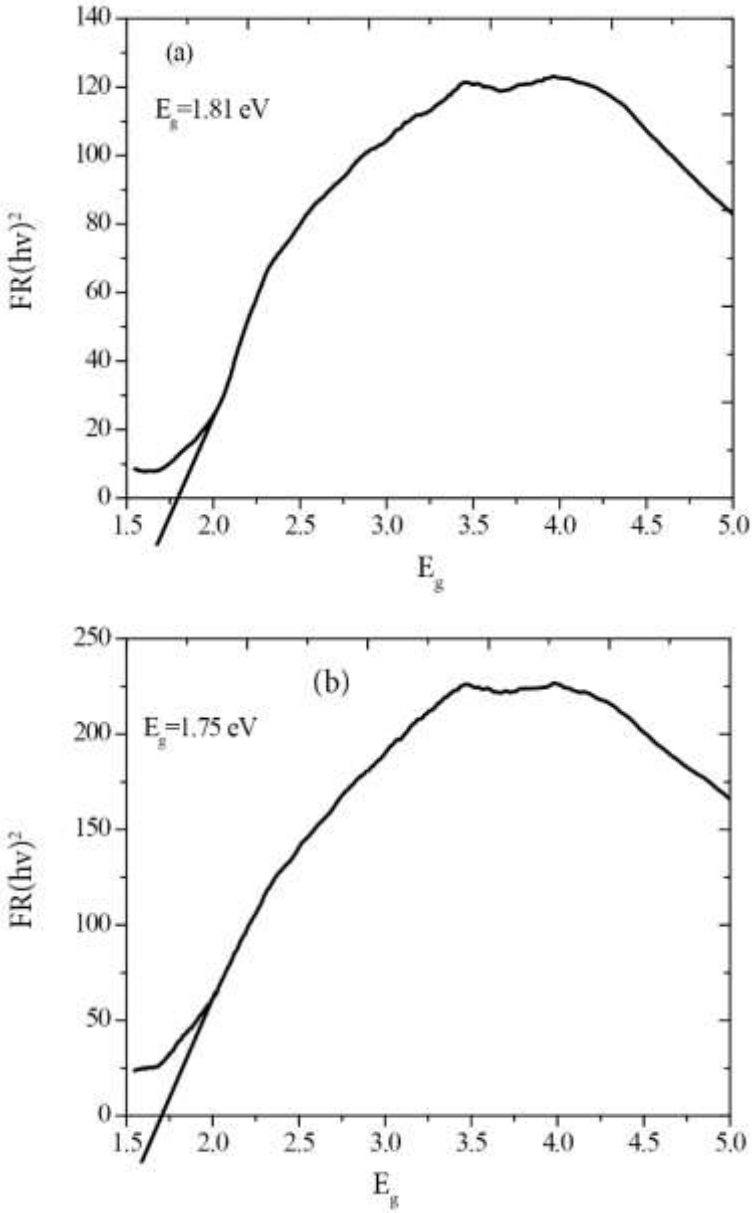

Figure 6. Band gap spectra of $ZnFe_{2-x}Al_xO_4$ (x = 0 and 0.5) nanoparticles.

A plot of $(F(R)h\nu)^2$ Vs hν was constructed for $ZnFe_2O_{-x}Al_xO_4$ (x = 0 and 0.5) nanoparticles (Figure 6). The extrapolation of the linear region of the Tauc plot revealed optical bandgap energies of 1.81 eV for x = 0 and 1.75 eV for x = 0.5. The reduction in optical bandgap with decreasing crystallite size indicates the occurrence of quantum confinement effects at the nanoscale, as reported in previous studies are well matched with the present study [18-20]. The tunability of the optical bandgap in these spinel ferrites makes them promising candidates for optoelectronic and photonic functionalities when integrated into polymer matrices, particularly for applications requiring tailored absorption in the visible region such as solar harvesting, sensors, and optical limiting components in composite systems.

Fourier Transform Infrared Spectroscopy Analysis

The vibrational modes and functional groups present in the $ZnFe_2O_{-x}Al_xO_4$ nanoparticles are investigated within the mid-infrared region (400-4000 cm^{-1}), using FTIR offering valuable information on metal-oxygen bonding.

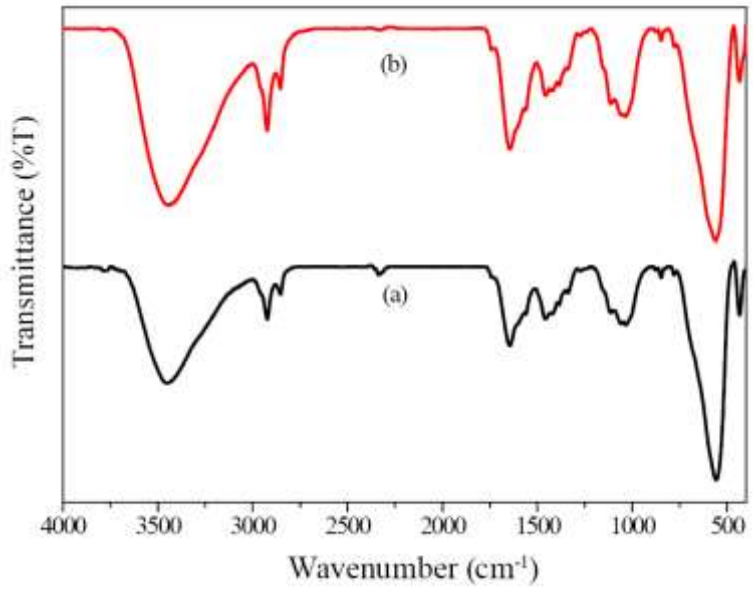

Figure 7. FTIR spectra of $ZnAl_xFe_{2-x}O_4$ (x = 0 and 0.5) nanoparticles.

Figure 7 presents the FTIR spectra of synthesized $ZnFe_2O_{-x}Al_xO_4$ (x = 0 and 0.5) nanoparticles with varying molar ratios. The spectra exhibit characteristic peaks at 3781, 3441, 2854, 2329, 1744, 1644, 1562, 1459, 1337, 1112, 1037, 850, 775, 578, and 437 cm^{-1}, confirming the formation of $ZnFe_2O_{-x}Al_xO_4$ nanoparticles. Specifically, the peak at 578 cm^{-1} is attributed to Zn-O bond formation, while the peak at 437 cm^{-1} is assigned to Fe-O bond formation. The peaks at 3781, 3441, 2854, 2329, 1744, 1644, 1562, 1459, and 1337 cm^{-1} are associated with the stretching and bending vibrations of hydroxyl (-OH) groups present in the sample [21-25]. Notably, the incorporation of Al ions causes a mild shift in the peak positions, indicating a significant impact on the vibrational modes of the $ZnFe_2O_{-x}Al_xO_4$ nanoparticles. Importantly, slight shifts in vibrational band positions were observed upon Al^{3+} incorporation, indicating structural distortion and modification of local bonding environments. These shifts reflect the successful substitution of Al^{3+} into the lattice, influencing the metal–oxygen framework. Such variations in vibrational modes are critical when these nanoparticles are used as fillers in polymer composites, as they affect the potential for interfacial interactions, hydrogen bonding, and dispersion within polymer matrices, key factors that determine the mechanical, dielectric, and barrier properties of nanocomposite systems.

Magnetization analysis

The magnetic properties of $ZnFe_2O_{-x}Al_xO_4$ (x = 0 and 0.5) nanoparticles were investigated at 300 K, with an applied magnetic field ranging from -15 kOe to +15 kOe. From the hysteresis loops (Figure 8) the values of remanence magnetization (Mr), coercivity (Hc), and saturation magnetization (Ms) were extracted to evaluate their potential for incorporation into polymer-based magnetic composites. The $ZnFe_2O_{-x}Al_xO_4$ (x = 0 and 0.5) spinel nanoparticles exhibited a normal spinel structure, where divalent Zn^{2+} ions occupy tetrahedral sites and trivalent Fe^{3+} ions occupy octahedral sites. The nanoparticles demonstrated ferromagnetic behavior.

The coercivity values for $ZnFe_2O_{-x}Al_xO_4$ (x = 0 and 0.5) nanoparticles were 238 Oe and 371 Oe, respectively. The coercivity is primarily influenced by factors such as high anisotropy, cationic redistribution, and surface defects in the nanoparticles. The hysteresis loop analysis yielded Mr values of 0.81 emu/g and 2.03 emu/g for $ZnFe_2O_{-x}Al_xO_4$ (x = 0 and 0.5) nanoparticles, respectively. The Ms values obtained from the hysteresis plots were 2.86 emu/g and 9.07 emu/g for $ZnFe_2O_{-x}Al_xO_4$ (x = 0 and 0.5) nanoparticles, respectively [26-28]. These variations are attributed to nanoscale effects, particle morphology, and cationic redistribution within the spinel lattice. The observed soft

ferromagnetic nature, combined with tunable magnetic parameters (Table 2), suggests that these

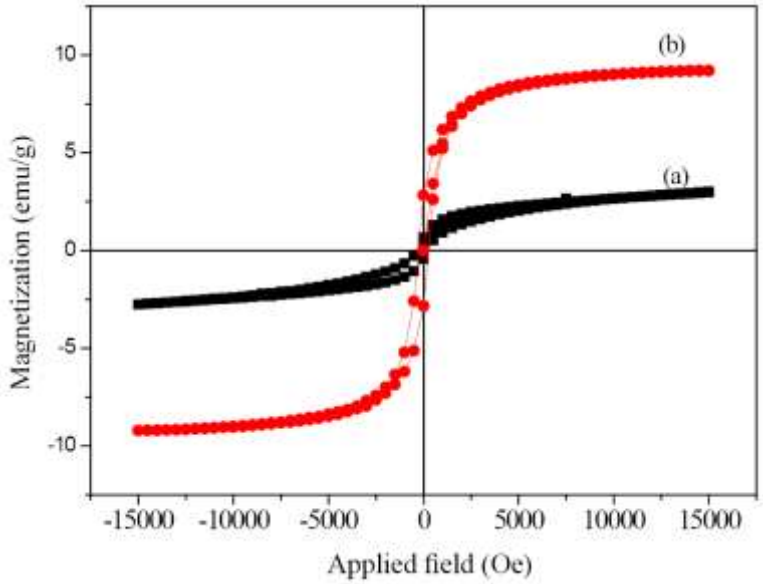

Figure 8. VSM spectra of $ZnFe_{2-x}Al_xO_4$ (x = 0 and 0.5) nanoparticles.

Table 2. Coercivity, M_s and M_r of $ZnFe_{2-x}Al_xO_4$ (x = 0.0 and 0.5) samples.

Sample	Sample code	Coercivity (Oe)	M_s (emu/g)	M_r (emu/g)
$ZnFe_2O_4$	a	238	2.86	0.82
$ZnFe_{1.5}Al_{0.5}$ Fe_2O_4	d	371	9.07	2.03

nanoparticles are promising candidates for use as magnetic fillers in polymer composites designed for electromagnetic interference (EMI) shielding, magnetic sensing, or microwave absorption. Their integration into polymer matrices can enhance the multifunctional performance of advanced composite materials, particularly in smart and flexible electronic applications.

CONCLUSIONS

$ZnFe_2O_{-x}Al_xO_4$ nanoparticles (x = 0 and 0.5) were synthesized using the combustion method, resulting in single-phase spinel structures with a cubic crystal system. Powder X-ray diffraction (XRD) confirmed the formation of zinc ferrite, while energy-dispersive X-ray spectroscopy (EDAX) verified the presence of key elements. Field emission scanning electron microscopy (FE-SEM) revealed spherical, flake-like morphologies, with crystallite sizes calculated using the Debye-Scherrer formula. Spectroscopic analysis revealed the optical and vibrational properties of the nanoparticles. Estimated bandgap values suggested a quantum confinement effect at the nanoscale. Fourier transform infrared (FT-IR) spectroscopy confirmed metal-oxygen bonding, such as Zn-O and Fe-O. Magnetic characterization showed ferromagnetic behavior, with saturation magnetization, coercivity, and remanence magnetization values calculated from hysteresis curves. These findings demonstrate the potential of Al-doped $ZnFe_2O_4$ nanoparticles as multifunctional fillers in polymer-based composite systems for magnetic sensing, EMI shielding, and spintronic applications. The tunable optical and magnetic properties make these materials highly suitable for next-generation smart composite materials with integrated magnetic and optical functionalities.

REFERENCES

1. Ibrahim, Abed Alqader, Marwan Saed, et al. Magnetic zinc ferrite nanostructures: Recent advancements for environmental and biomedical applications. *J. Alloys Compd.* 2024; 4: 100038p.

2. Azouzi, Wafaa, Ikram Boulahya, et al. Ultrasonic chemical synthesis of zinc-manganese ferrites with improved magnetic properties. *Ultrason. Sonochem.* (2024); 111: 107108p.
3. Thakur, Deepika, Mamta Latwal, et al. Zinc ferrite nanoparticles and their biomedical applications. *Oxides for medical applications*. 2023; 233-255p.
4. Latif, Shoomaila, Amna Liaqat, et al. Development of zinc ferrite nanoparticles with enhanced photocatalytic performance for remediation of environmentally toxic pharmaceutical waste diclofenac sodium from wastewater. *Environ. Res.* (2023); 216: 114500p.
5. Nigam, Abhishek, Sheetal Saini, et al. Zinc doped magnesium ferrite nanoparticles for evaluation of biological properties viz antimicrobial, biocompatibility, and in vitro cytotoxicity. *Mater. Today Commun*. 2022; 31: 103632p.
6. Boon, M. S., WP Serena Saw, et al. Magnetic, dielectric and thermal stability of Ni–Zn ferrite-epoxy composite thin films for electronic applications. *J. Magn. Magn. Mater. 2012;* 324(5): 755-760 p.
7. Gautam, Sanjeev, Ritika Charak, et al. Tailoring magnetism in chromium-doped zinc cobalt ferrite nanostructure for advanced spintronic memory devices. *Mater. Today Chem. 2024;* 41: 102291p.
8. Muthusamy, Athianna, Vajaravel Jawahar, et al. Preparation, electrical and magnetic properties of poly (m-phenylenediamine)/ZnFe2O4 nanocomposites. *J. Supercond. Nov. Magn.* 2018; 31(2): 497-504p.
9. Almeshaal, Mohammed, Sivasubramanian Palanisamy. Physico-chemical characterization of Grewia Monticola Sond (GMS) fibers for prospective application in biocomposites. *J. Nat. Fibers*. 2022; 19(17). 15276-15290.
10. Padmanabhan, R. G, S. Rajesh, et al. Evaluation of mechanical properties and Fick's diffusion behaviour of aluminum-DMEM reinforced with hemp/bamboo/basalt woven fiber metal laminates (WFML) under different stacking sequences. *Ain Shams Eng. J*. 2024; 15(7). 102759.
11. Ahmad, Yaseen, Tariq Mustafa, et al. Calcium (Ca) and dysprosium (Dy) co–doped spinel zinc ferrite: Synthesis, multifunctional properties and its applications. *Inorg. Chem. Commun.* 2023; 158: 111484p.
12. AMahmood, Aamir, Asghari Maqsood. Temperature and frequency-dependent electrical transport studies of manganese-doped zinc ferrite nanoparticles. *Mater. Sci. Eng. B.* 2023; 296: 116615p.
13. Palanisamy, Sivasubramanian, Mayandi Kalimuthu, et al. Wear properties and post-moisture absorption mechanical behavior of kenaf/banana-fiber-reinforced epoxy composites. *Fibers*. 2022; 10(4). 32.
14. Palaniappan, Murugesan, Sivasubramanian Palanisamy, et al. Synthesis and suitability characterization of microcrystalline cellulose from Citrus x sinensis sweet orange peel fruit waste-based biomass for polymer composite applications. *J. Polym. Res*. 2024; 31(4).105.
15. Goutham, Emani Ram Sai, Shaik Sajeed Hussain, et al. Drilling parameters and post-drilling residual tensile properties of natural-fiber-reinforced composites: A review. *J. Compos. Sci*. 2023; 7(4). 136.
16. Hoque, S. Manjura, Md Sazzad Hossain, et al. Synthesis and characterization of ZnFe2O4 nanoparticles and its biomedical applications. *Mater. Lett.* 2016; 162: 60-63p.
17. Tamhankar, Prasad M, Aparna M. Kulkarni, et al. Functionalization of cobalt ferrite nanoparticles with alginate coating for biocompatible applications. *Mater. Sci. Appl.* 2011; 9(2): 1317-1321p.
18. Alsalmah, Hessa A, A. Rajeh. Optical, conductivity, dielectric, and magnetic properties of polymer nanocomposite based on PAM/cs matrix and ZnFe2O4 NPs for use in magneto-electronic and energy storage capacitor devices. *Ceram. Int.* 2024; 50(7): 12167-12174p.
19. Ramadan, Rania, Vuk Uskoković, et al. El-Masry. Triphasic CoFe2O4/ZnFe2O4/CuFe2O4 nanocomposite for water treatment applications. *J. Alloys Compd.* 2023; 954: 170040p.
20. Kurian, Jessyamma, M. Jacob Mathew, et al. Structural, optical and magnetic studies of CuFe2O4, MgFe2O4 and ZnFe2O4 nanoparticles prepared by hydrothermal/solvothermal method. *J. Magn. Magn. Mater*. 2018; 451: 121-130p.

21. Pradeep, A., G. Chandrasekaran, et al. FTIR study of Ni, Cu and Zn substituted nano-particles of MgFe2O4. *Mater. Lett*. 2006: 60(3) 371-374p.
22. Pradeep.A, P. Priyadharsini, G. Chandrasekaran. Sol–gel route of synthesis of nanoparticles of MgFe2O4 and XRD, FTIR and VSM study. *J. Magn. Magn. Mater*. 2008; 320(21): 2774-2779p.
23. El-Masry, Mai M., Mahmoud El-Shahat, Rania Ramadan, Reda M. Abdelhameed, et al. Selective photocatalytic reduction of nitroarenes into amines based on cobalt/copper ferrite and cobalt-doped copper ferrite nano-photocatalyst. *J. Mater. Sci.: Mater. Electron*. 2021; 32(13): 18408-18424p.
24. Larumbe. S, J. I. Perez-Landazabal, J. M. Pastor. Sol-gel NiFe2O4 nanoparticles: Effect of the silica coating. *J. Appl. Phys.* 2012; 111(10).
25. Li, Yongbo, Ran Yi. Facile synthesis and properties of ZnFe2O4 and ZnFe2O4/polypyrrole core-shell nanoparticles. *Solid State Sci.* 2009; 11(8): 1319-1324p.
26. Jacinto, M. J., L. F. Ferreira. Magnetic materials for photocatalytic applications a review. *J. Sol-Gel Sci. Technol.* 2020; 96(1): 1-14p.
27. Bhattu, Monika, Roberto Acevedo. A comprehensive review on the synthesis routes, properties and potential applications of ZnFe2O4 ferrites. In *E3S Web of Conferences*. 2024; 588: 02014p.
28. Deepty. M, Srinivas. C, N. Krishna Mohan, et al. Chemical synthesis of Mn–Zn magnetic ferrite nanoparticles: Effect of secondary phase on extrinsic magnetic properties of Mn–Zn ferrite nanoparticles. *Ceram Int.* 2024; 50(11): 18446-18453p.

